

Hydrogen Fires

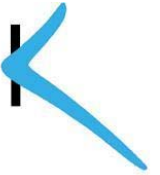
Jennifer X Wen

Fire and Explosion Research Group

Faculty of Engineering, Kingston University

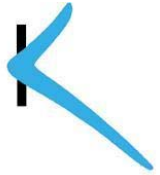
London, UK

Outline (Lecture 2)



- **Thermodynamic properties of hydrogen**
- **The underexpanded hydrogen jets and jet fires**
- **Numerical prediction of hydrogen jet fires from high pressure releases**
- **Pool spreading, vaporization and burning of a liquid hydrogen (LH2) spill**

Thermodynamic properties of hydrogen



- The properties of hydrogen at high pressure deviate from that of the ideal gas

- The Van der Waals equation of state

$$\left(P + \frac{a(p)}{V_m^2}\right)(V_m - b(p)) = RT$$

- The Abel-Noble equation of state

$$\rho = P/(RT + bP)$$

valid for $P < 1600 \text{ atm}$ and $T > 200 \text{ K}$

Comparison of different EoS

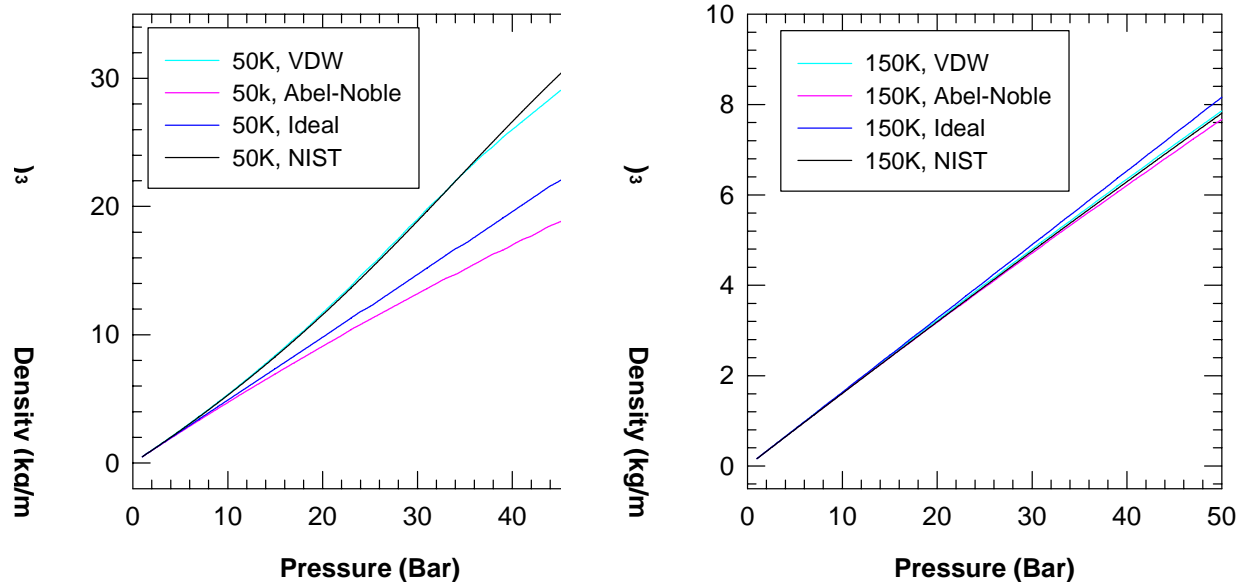
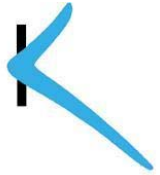
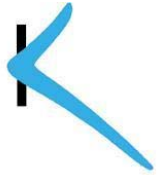


Fig. 34 Comparison of density versus pressure for temperatures calculated using the Van der Waals (VDW) and Abel-Noble real gas EoS, and the ideal gas EoS, as well as the tabulated data from NIST (reproduced from [76]).

The Joule-Thomson effect



- Most gases at ambient temperatures cool when expanded across a porous plug. However, the temperature of hydrogen increases when the gas is expanded at a temperature above its inverse Joule-Thomson temperature 193 K (-112 °F).

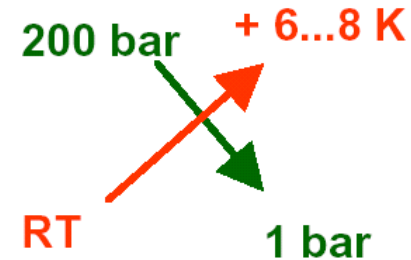
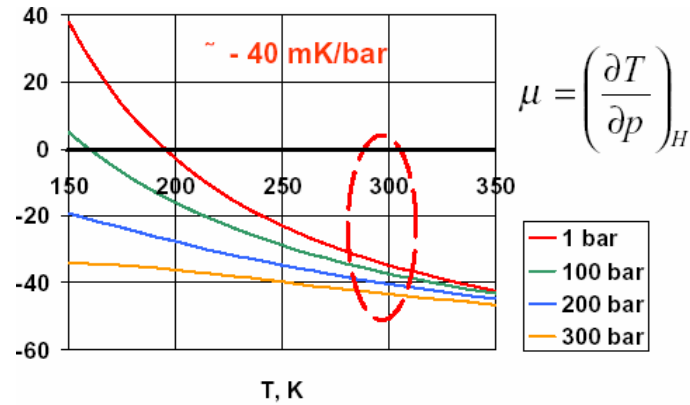


Fig. 36 Negative Joule-Thomson coefficient (reproduced from [52])

Underexpanded hydrogen jets – the physical process immediately following the release

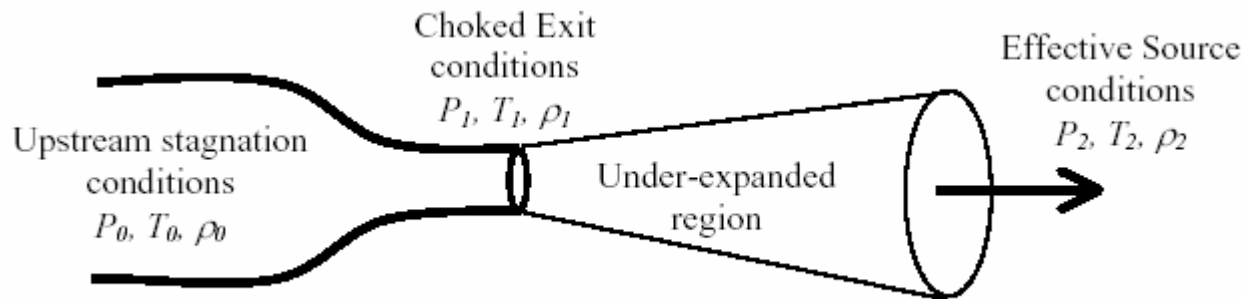


Fig. 37 Schematic of jet development under choked flow conditions (reproduced from [61]).

Underexpanded hydrogen jets – the physical process immediately following the release

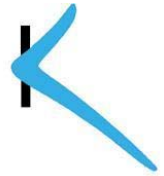
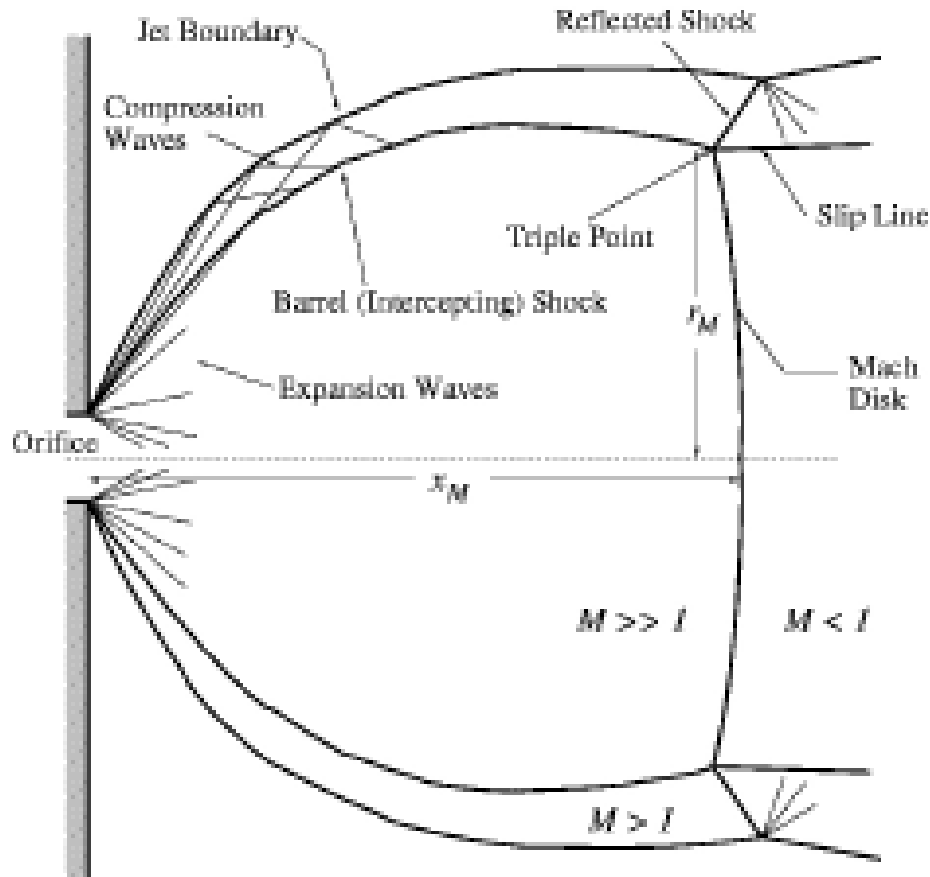


Fig. 38 Schematic of the shock structure (reproduced from [60])



Two Modelling Approaches

- **Pseudo-source** approach (Ewan and Modie 1985)

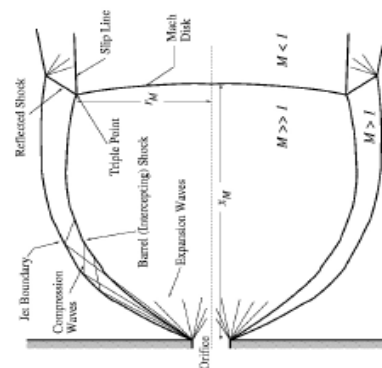
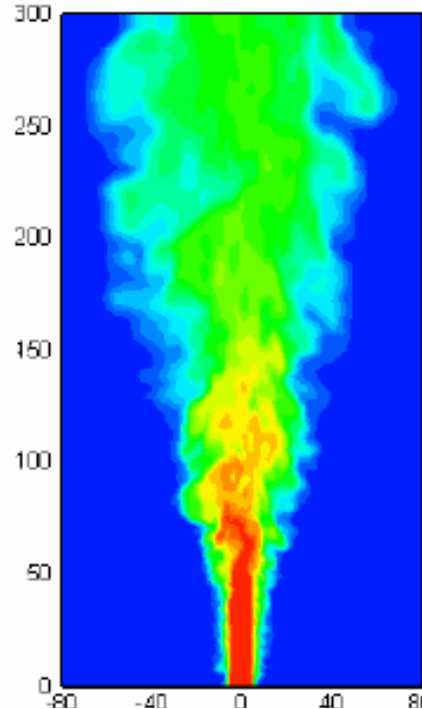
– Leak modelled from downstream as a sonic jet with the same mass flow rate

$$D_{eq} = D_j (0.536 C_D \frac{P_o}{P_a})^{0.5}$$

$$P_e = P_o \left(\frac{2}{\gamma + 1} \right)^{\gamma / \gamma - 1}$$

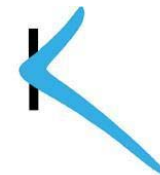
$$\rho_e = \rho_o \left(\frac{2}{\gamma + 1} \right)^{\gamma / \gamma - 1}$$

$$Y_o = \frac{4.99 D_s}{z} \left(\frac{\rho_g}{\rho_a} \right)^{1/2} C_D^{1/2}$$

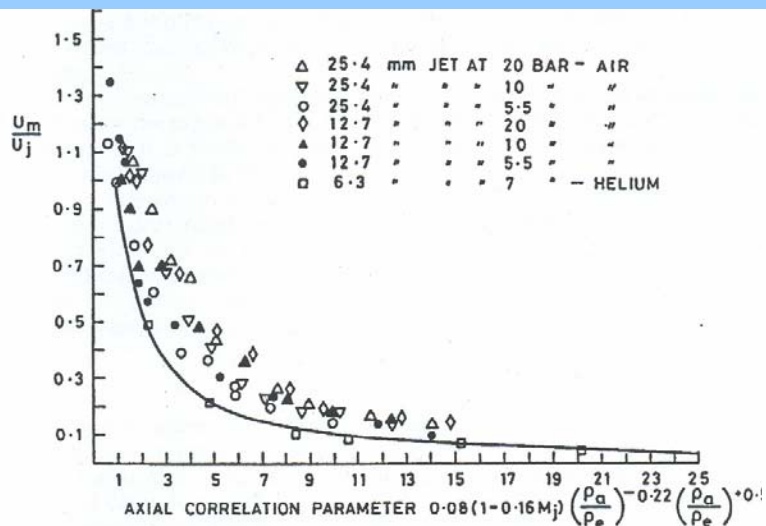


- **Numerically** solving the under-expanded shock structure
- Results used as inflow for the subsequent large eddy simulation of the jet

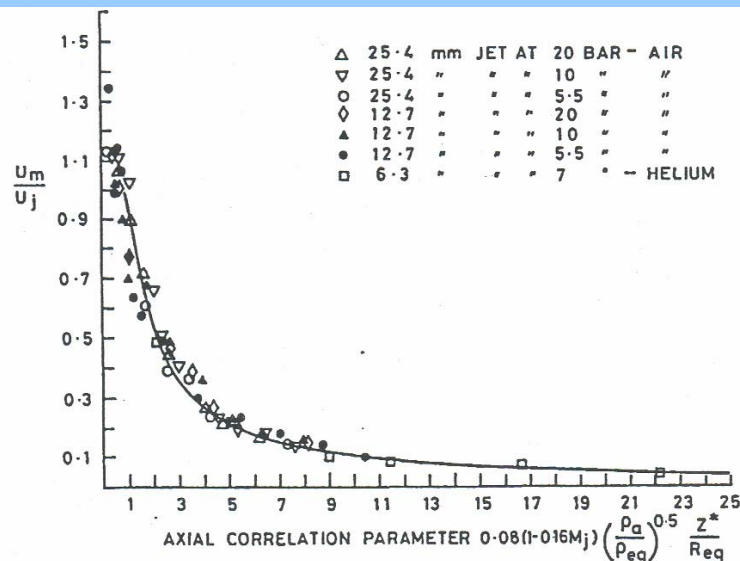
Rationale behind the pseudo-source approach



- A suitable model for the underexpanded jets redefines a new jet at a point downstream which is fully expanded

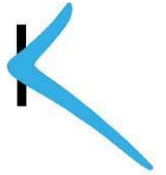


Centreline axial velocity decay using eddy viscosity coefficient due to Witze at indicated stagnation pressures. (reproduced from [60]).



Centreline axial velocity decay using Warren parameter with corrected axial origin as indicated stagnation pressures (reproduced from [60]).

Numerically resolving the under-expanded shock structure



- A major limitation of the Pseudo approach is that it can not take into account the air entrainment into the hydrogen jet. An alternative approach is to numerically resolve the complex under-expanded shock structure.
- Very few numerical studies were concerned with the highly underexpanded hydrogen jet into an atmospheric environment

CFD predictions of highly underexpanded air and nitrogen jets (Cumber et al. [66])

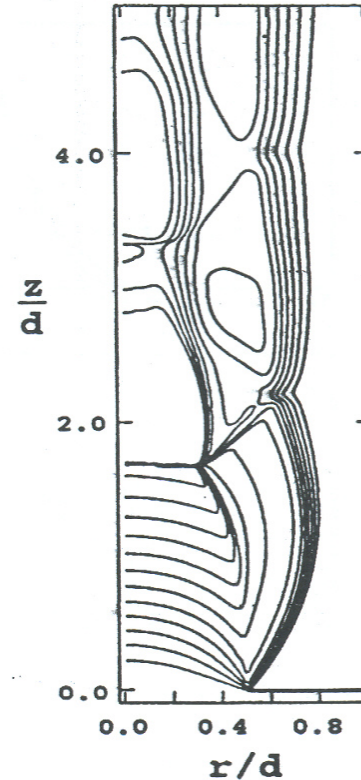
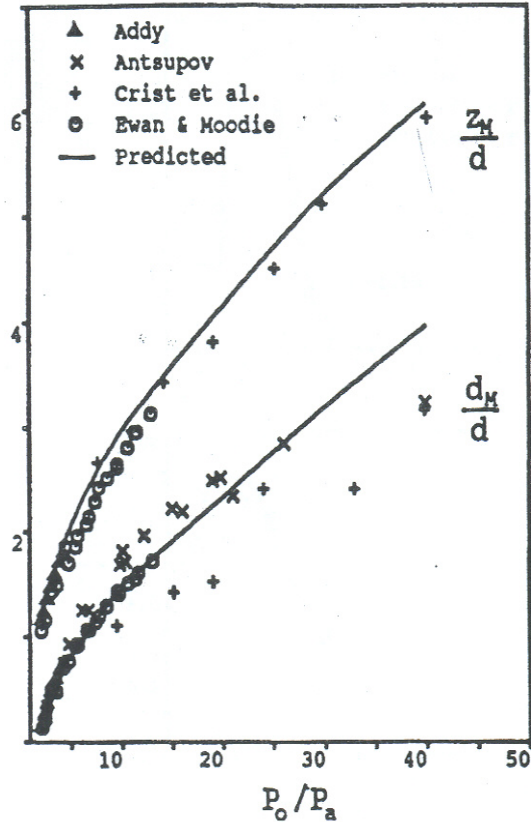
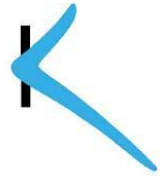


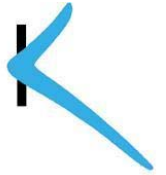
Fig. 44 Predicted Mach number contours within the near field region of Donaldson and Snedeker's [73] air jet ($d=13\text{mm}$, $P_e/P_a=3.57$, $M=1$).

Variation of dimensionless Mach disc diameter and stand-off distance with pressure ratio (reproduced from [66]).

Simulation of the Under-expanded Shock Structure in Hydrogen Jets (Xu et al. [75] and Zhang et al. [76])

- **Commercial code CFX**
 - Total energy model take into the kinetic energy of high speed flows
 - The $k-\omega$ based shear stress turbulence (SST) model
 - A TVD type high resolution discretisation scheme to represent sharp gradients without numerical oscillations
 - A global 2nd accuracy, which switches to a 1st order upwind scheme locally to prevent non-physical oscillations
 - The 2nd order backward Euler scheme to define the discretisation algorithm for the transient term.

Choked Flow Nozzle Dynamics



- Assuming isentropic flow

$$P^* = P_o \left(\frac{2}{\gamma + 1} \right)^{\frac{\gamma}{\gamma - 1}}$$

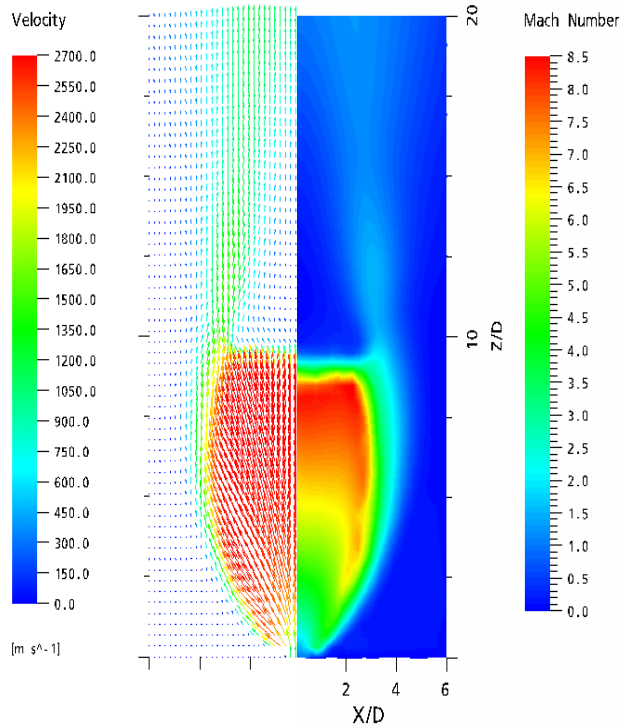
$$\rho^* = \rho_o \left(\frac{2}{\gamma + 1} \right)^{\frac{1}{\gamma - 1}}$$

- T* from Van der Waals EoS

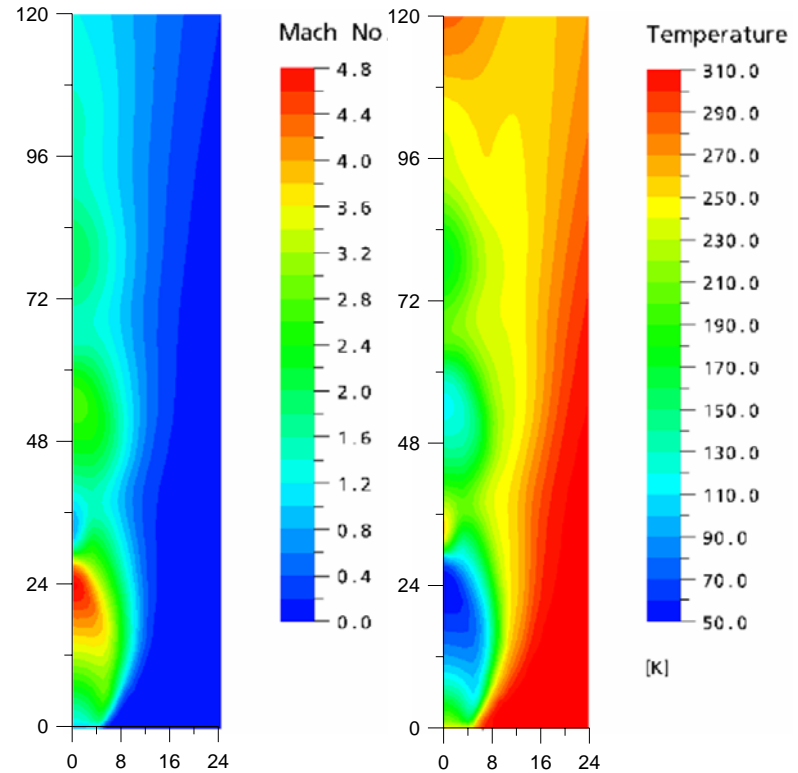
Table 1. Initial data in the high-pressure jet simulation

Vessel pressure (MPa)	20
Release temperature (K)	267
Vessel temperature (K)	300
Release velocity (m/s)	1020
Orifice diameter (m)	0.01
Discharge coefficient	0.85
Release pressure (MPa)	10.6
Density in the vessel (Kg/m3)	14.1
Density at nozzle exit (kg/m3)	8.93

Comparison of the simulated 200 bar and 20 bar hydrogen jets

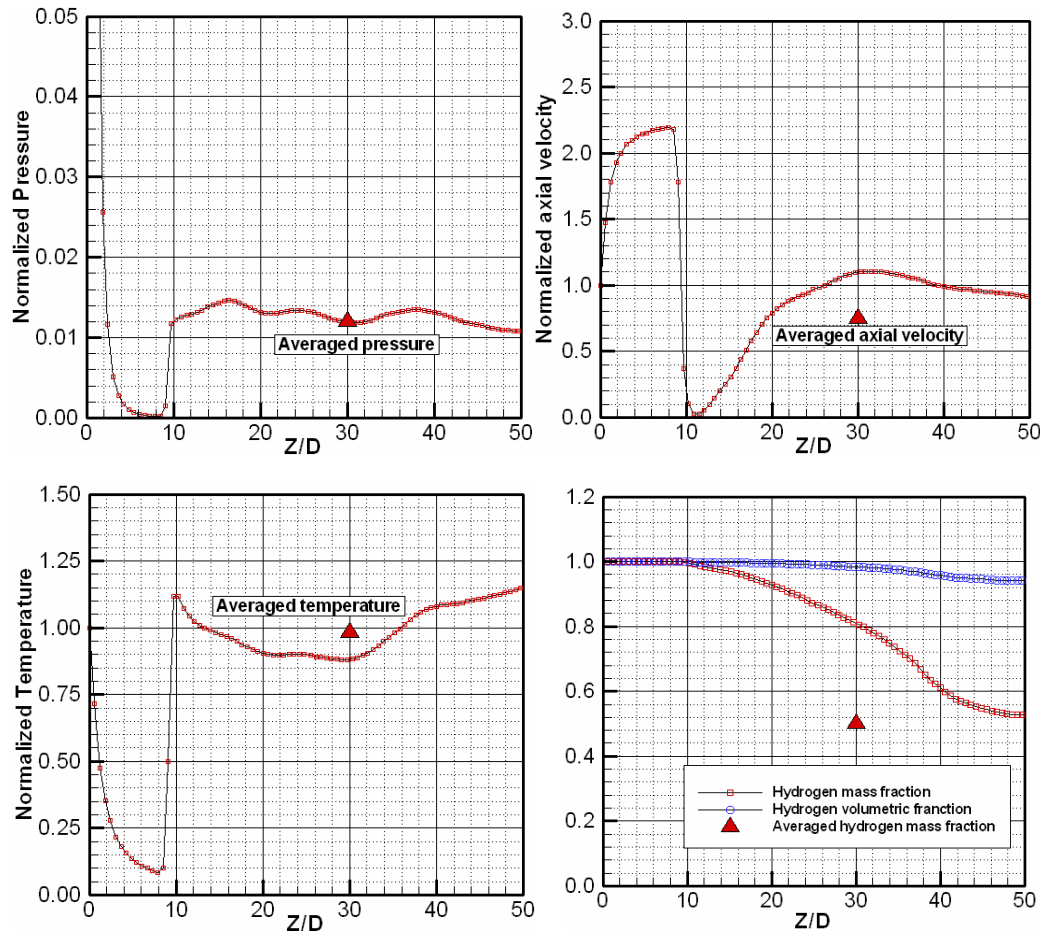
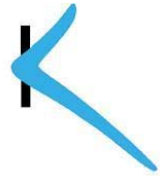


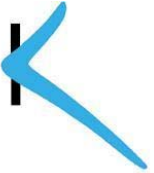
Vector of velocity and contour of Mach number in the 200 bar simulation (reproduced from [75])



Mach number and temperature in the 20 bar simulation. (reproduced from [76])

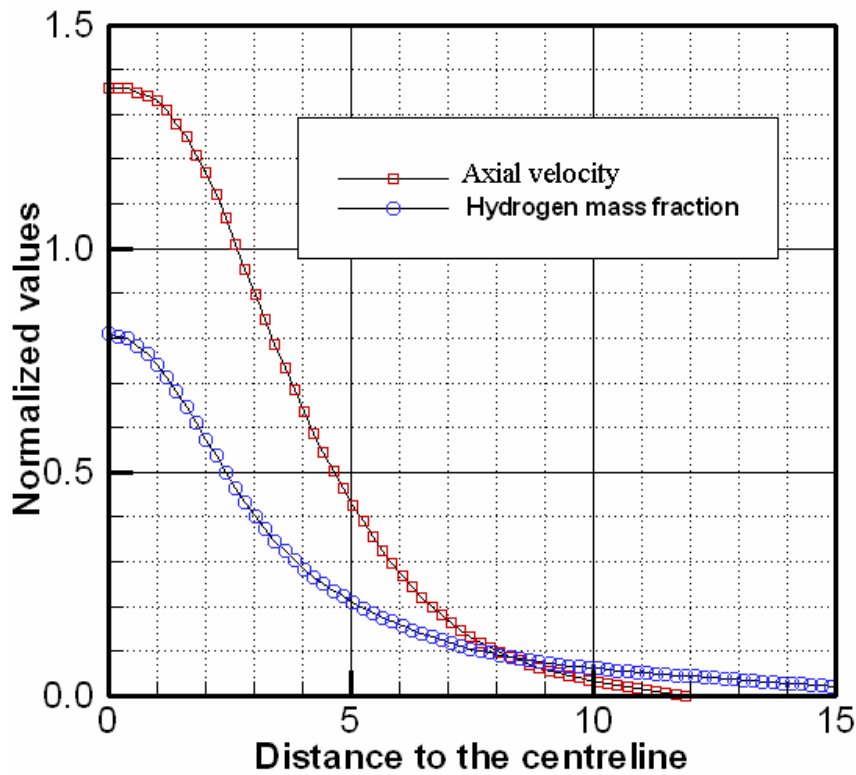
The predictions for the normalized pressure, axial velocity and temperature as well as the hydrogen mass and volumetric fractions on the centerline for the 200 bar hydrogen jet (reproduced from [75])



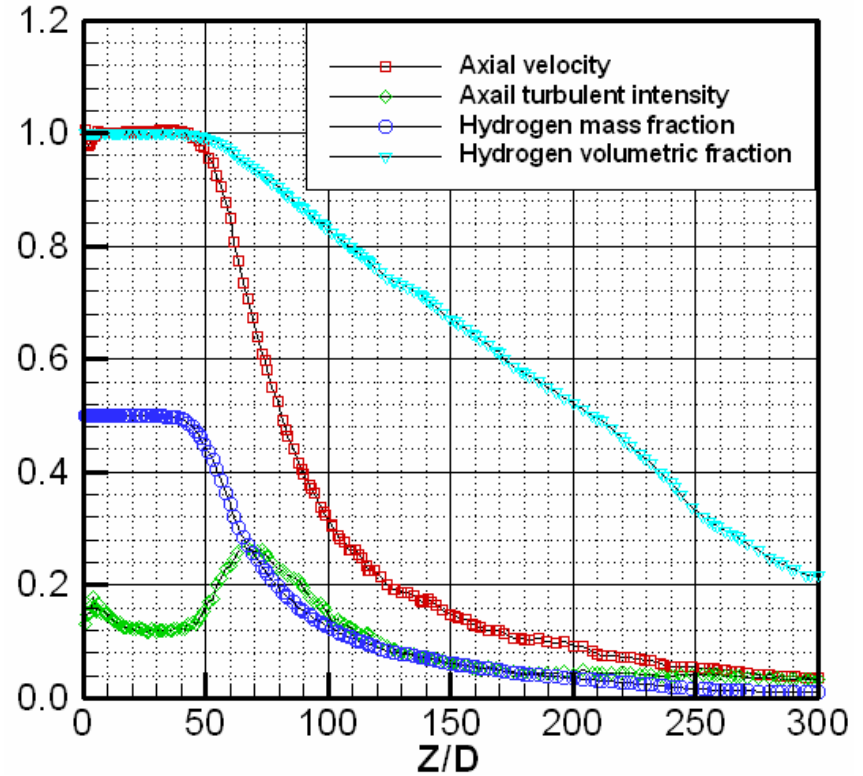


Predictions of the 200 bar hydrogen jet

(Xu et al. [75])



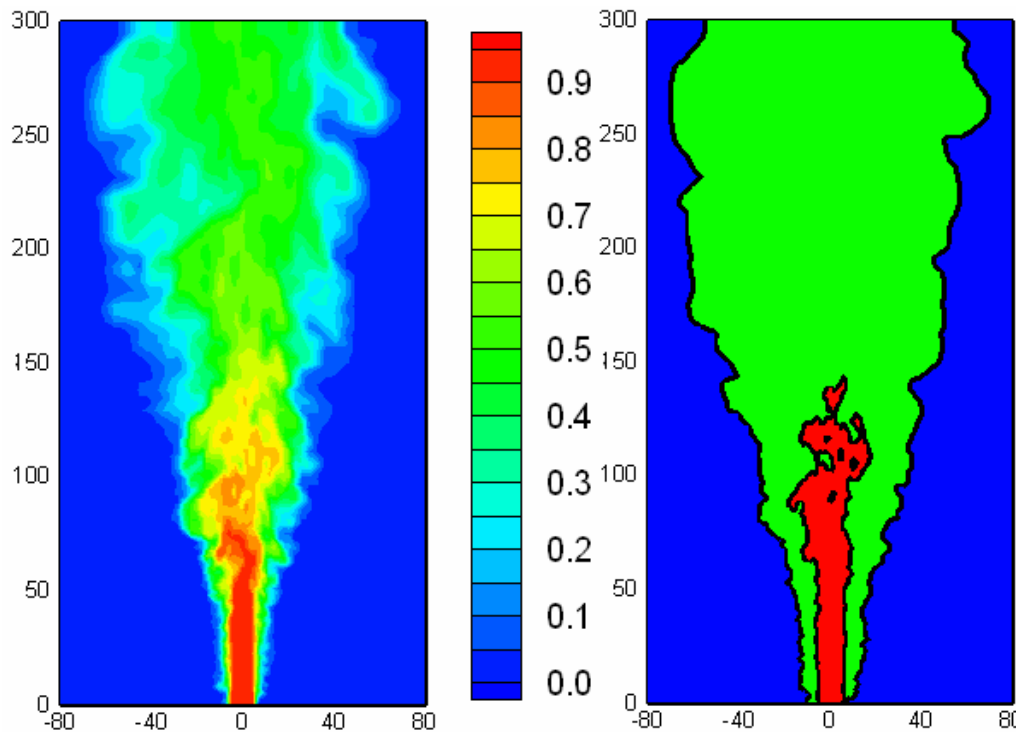
Axial velocity and hydrogen mass fraction versus distance to the centreline at $Z=30D$



Normalized values of main axial velocity, axial turbulent intensity and hydrogen mass fraction on the centerline

Predictions of the 200 bar hydrogen jet

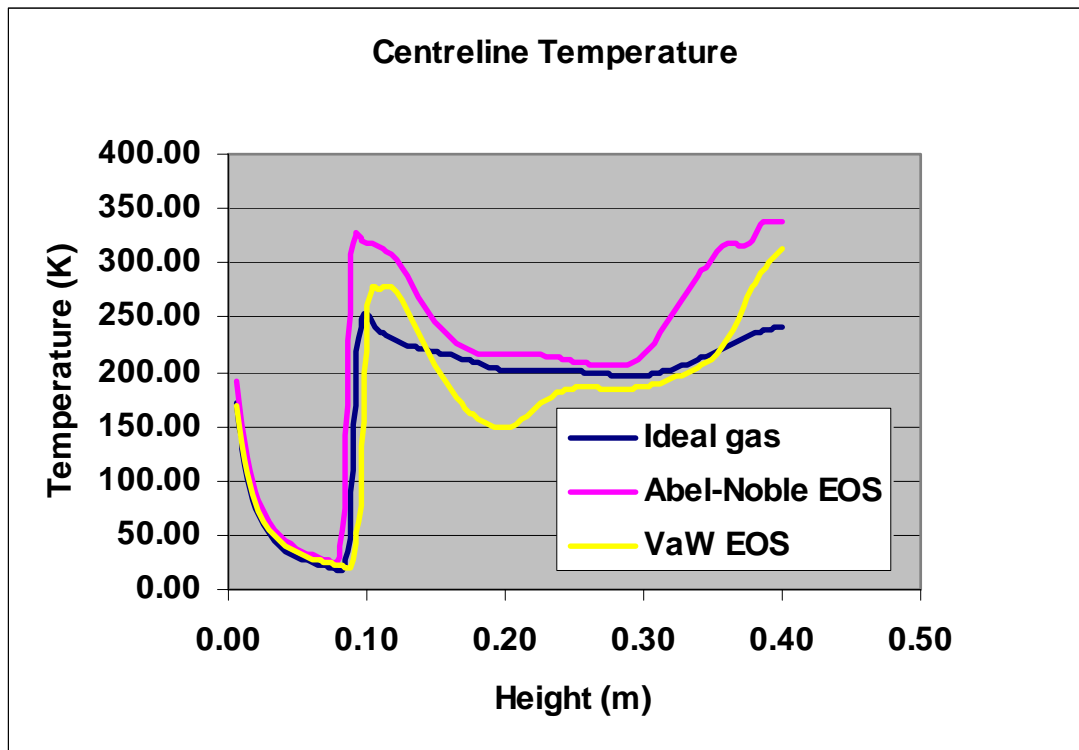
(Xu et al. [75])



Contour of hydrogen volumetric fraction (left) and flammable range (right) at $t=0.1s$ reproduced from [75]).

Predictions of the 200 bar hydrogen jet

(Xu et al. [75])



Comparison of the predicted centreline temperature distributions when different Equation of State is used

Numerical prediction of hydrogen jet fires from high pressure releases

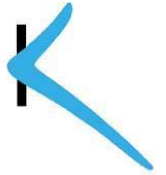
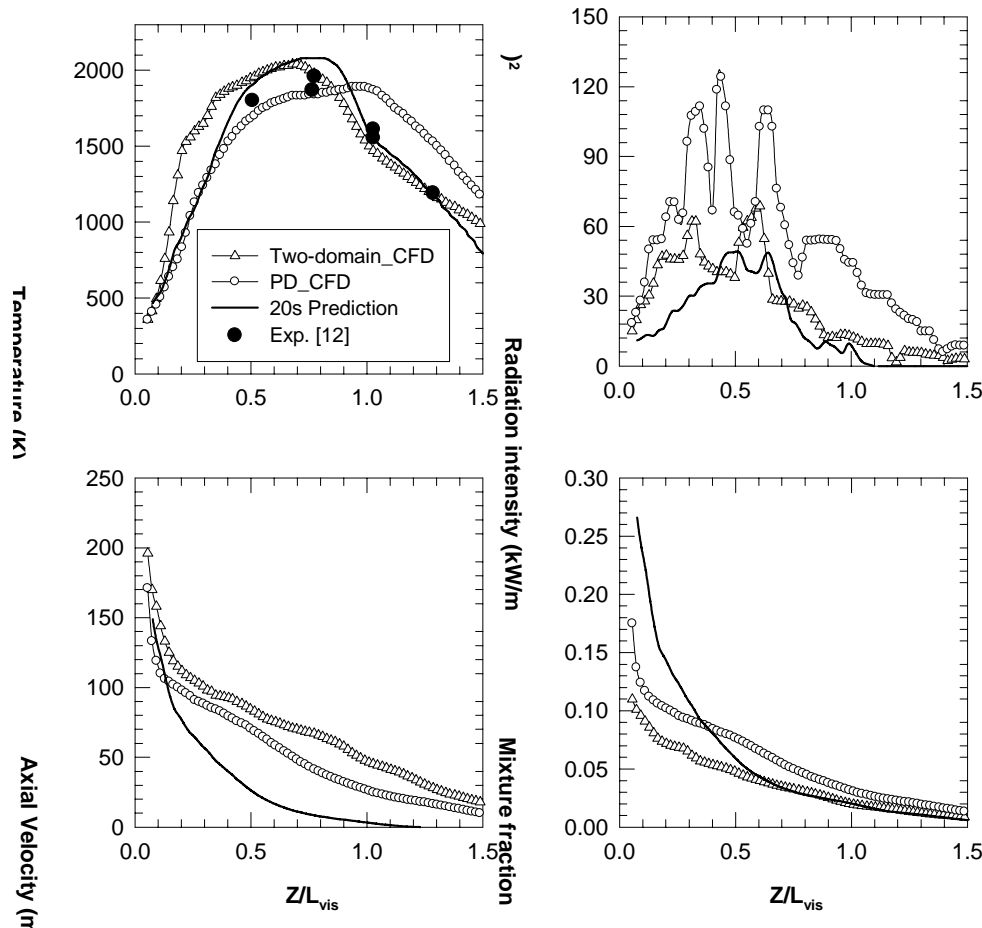


Table 13 Predictions of hydrogen jet flames by the Shell Fred model (reproduced from [38])

Orifice diameter (mm)	Release pressure (barg)	Mass flow rate (kg/s)	Length of visible flame (m)	Flame lift-off (m)	Total flame length (m)
6	70	0.1	5.9	1.2	7.1
3	50	0.018	3.0	0.6	3.6
3	100	0.035	3.9	0.8	5.7
3	130	0.045	5.3	0.9	5.2

Numerical prediction of hydrogen jet fires from high pressure releases

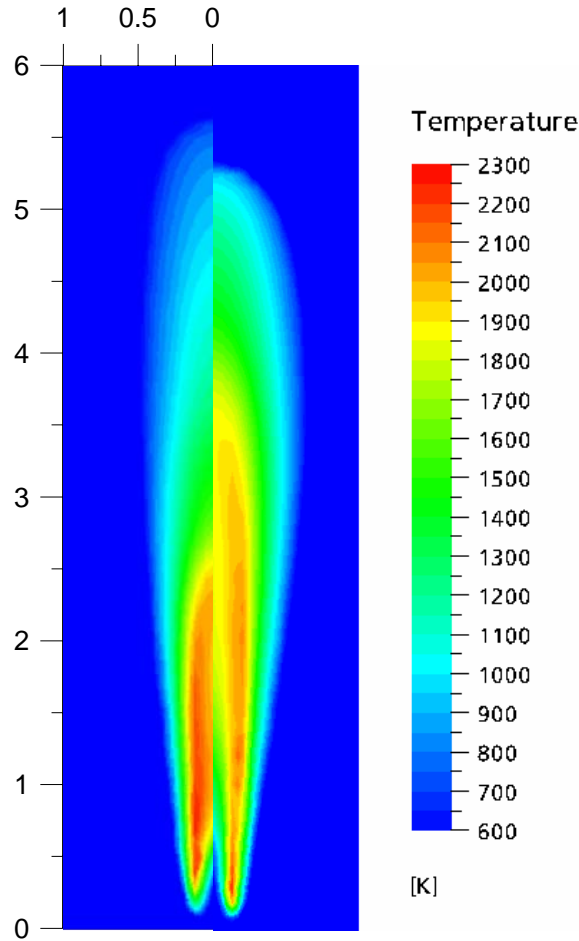
(Zhang et al. [76])



Comparison of the centreline temperature, incident intensity, axial velocity and mixture fraction predicted by the two-domain and pseudo approaches in the combustion simulations.

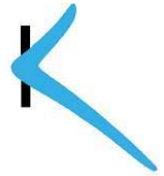
Numerical prediction of hydrogen jet fires from high pressure releases

(Zhang et al. [76])



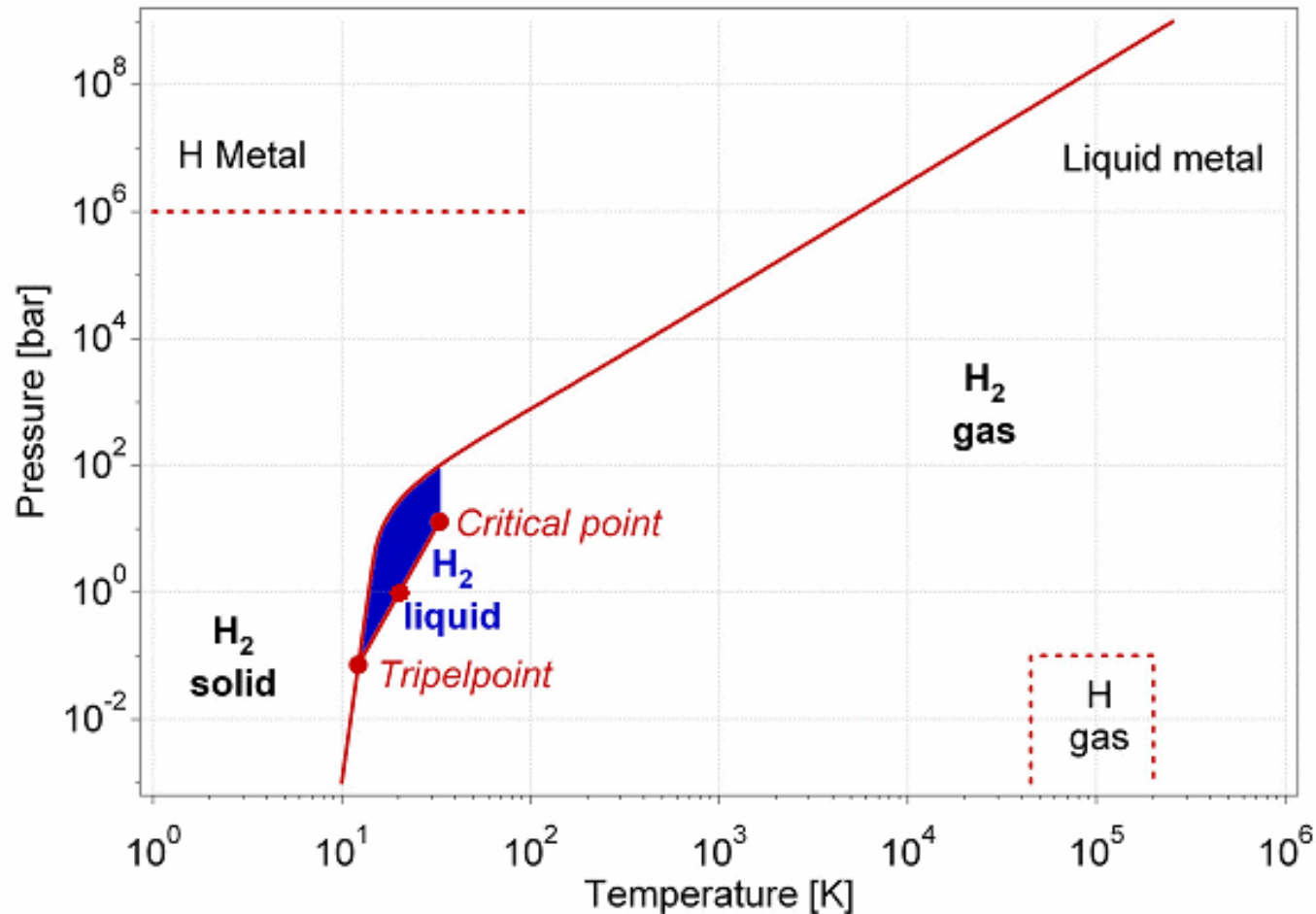
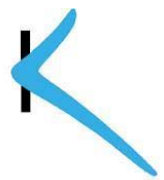
Contours of the predicted mean temperature by the two-domain approach (left) and the pseudo approach (right) in the combustion simulation. The field-of-view is 1m in the radial direction and 6m in the axial direction (reproduced from [76]).

Pool spreading, Vaporization and burning of a liquid hydrogen (LH2) spill



- LH2 release results in a liquid pool whose geometry is determined by its flow, i.e. type of release, flatness and pitch of the surface with which it interacts, and possible presence of obstacles.
- There is no well-defined or generic relation between the pool area and pool volume, except that the contact area will most likely increase with time.
- Most of the heat transfer is related to heating the vapour, not to producing it.

Liquid hydrogen typically has to be stored at 20K



Global analysis of LH2 spill

(Harstad and Bellan [87])

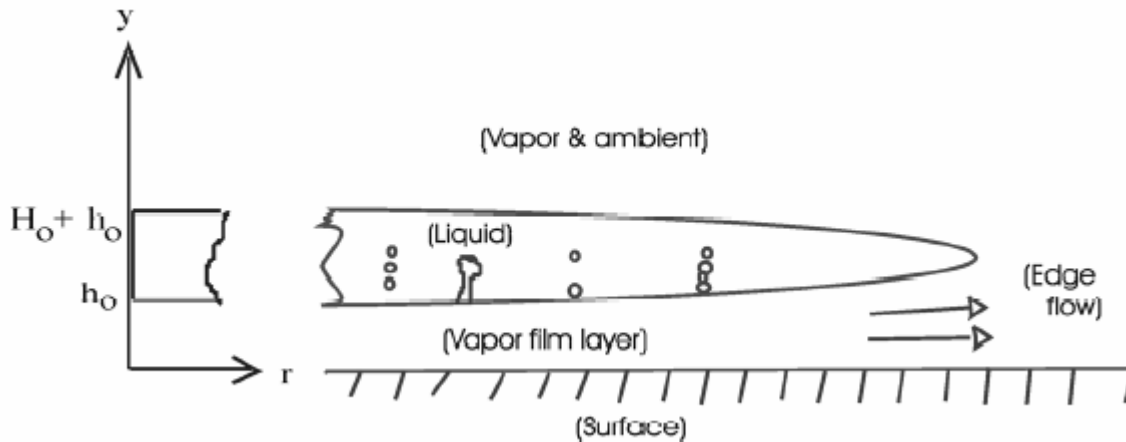
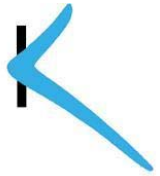
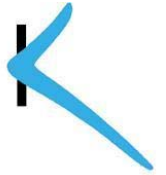


Fig. 55 Sketch of a LH2 pool (reproduced from [87]).

Global analysis of LH2 spill

(Harstad and Bellan [87])



Vaporization of a LH2 pool is produced primarily by film boiling and also possibly by radiant heating from flames above the pool.

The minimum pool evaporation time

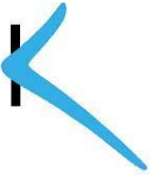
$$t_{\text{evap}} \approx [0.6 \text{ m}^2 \text{ s/kg}] M / A,$$

Characteristic circulation time within the burning cloud as a fireball

$$t_{\text{ref,conv}} \cong [0.5 \text{ bar}^{1/6} \text{ s/kg}^{1/6}] \left(\frac{M_c}{p_a} \right)^{1/6}$$

Global analysis of LH2 spill

(Harstad and Bellan [87])



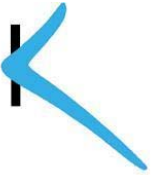
- **Estimation of the fireball produced by unconfined cloud releases of mass M_C :**

– size scales as: $L_{ref} \approx 7M_C^{1/3}$

– convection velocity as $u_{ref} \approx 14M_C^{1/6}$

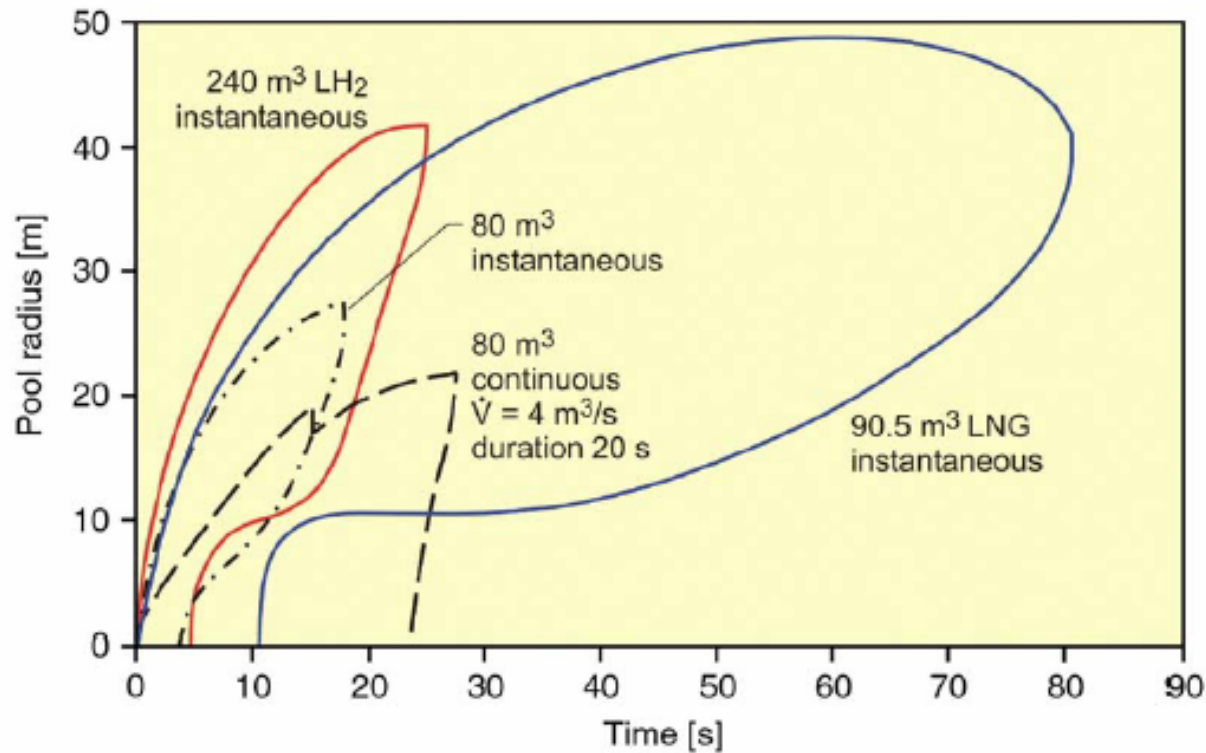
– The fireball lifetime: $3t_{ref,conv}$.

Numerical modelling LH2 spill



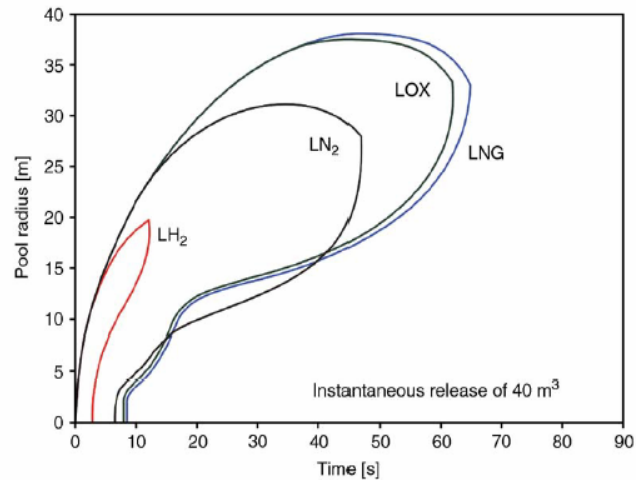
- **State-of-the-art modeling: shallow-layer equations**
 - Gravitational flow determined by the inertia of the cryogen and characterized by a hydraulic gradient at the front edge;
 - Gravitational viscous flow after pool height and spreading velocity have decreased making shear forces at the boundary dominant;
 - Equilibrium between surface tension and viscous forces and with gravitation being negligible.

Predictions of one large tank of LH2 in an instantaneous spill (Verfondern and Dienhart [86])

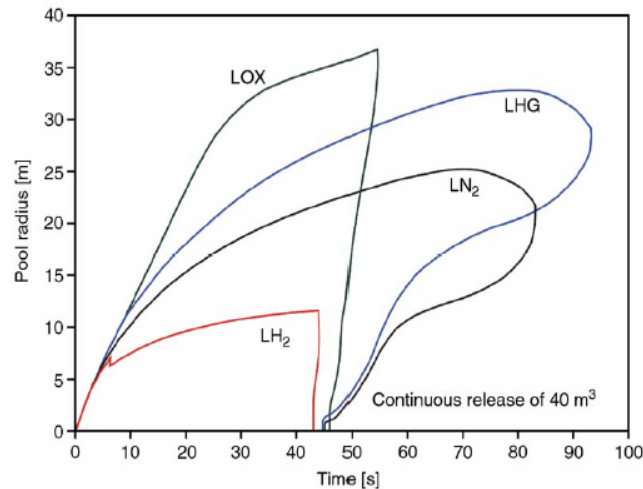


Instantaneous and continuous LH₂ release from Cryoplane fuel tank compared with an instantaneous LNG release of the same energy contents

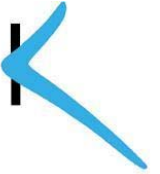
Predictions of one large tank of LH2 in an instantaneous spill (Verfondern and Dienhart [86])



Comparison of pool spreading behavior of 40m³ of four different cryogenics in an instantaneous release (top) and in a continuous release over 40 s (bottom)

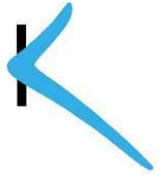


SLE and CFD



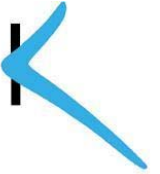
- **Limitation of SLE:** the calculations of the pool spreading is decoupled from the formation and subsequent dispersion of the combustible cloud while the former should be used to provide transient boundary conditions for the dispersion calculations
- **CFD** should help to achieve coupled predictions of the spreading, vapourisation and dispersion of LH2 spills for quantified risk assessment.

Summary



- **Limited attempts have been made in simulating very high pressure jets and even few in hydrogen jets and jet flames.**
- **Two modelling approaches can be used in the simulation of hydrogen jet fires. The pseudo source approach is computationally more efficient but seems to over predict the flame length and temperature. The predictions of the two-domain approach seems to be in better agreement with the limited amount of data available.**
- **It is important to use real gas equation of state in calculations involving high pressure hydrogen.**

Summary



- **By applying global analysis to liquid hydrogen spill, some useful estimation can be made on pool spreading, vaporization and burning of the resulting gaseous hydrogen cloud.**
- **The state-of-the-art on modelling liquid hydrogen spill is still the shallow layer equations. There is potential to develop CFD based approach for coupled predictions of the spreading, vapourisation and dispersion of LH2 spills.**
- **More experimental data, especially those at large scale, is needed to further our understanding of very high pressure hydrogen jets and aid the development and validation of predictive tools.**